International Journal of Biology and Life Sciences
ISSN: 2957-9511 | Vol. 15, No. 3, 2026

MiR-133b Targets FSCN1 to Inhibit the Malignant Progression of Oral Squamous Cell Carcinoma

Xinyue Chu, Peter Shaw *

Oujiang Laboratory (Zhejiang Lab for Regenerative Medicine, Vision and Brain Health), Wenzhou Medical University, Wenzhou, Zhejiang, China

*** Corresponding author:** Peter Shaw (Email: brighttale@163.com)

Abstract: Oral squamous cell carcinoma (OSCC) poses a significant challenge due to its aggressive nature and propensity for metastasis, leading to poor patient outcomes. Current treatment options for advanced-stage OSCC are limited, highlighting the urgent need for novel therapeutic approaches. In this context, microRNA-133b (miR-133b) has emerged as a promising candidate with tumor-suppressive properties across various cancer types, including OSCC. However, the specific mechanisms underlying its actions in OSCC have not been fully elucidated. To address this gap in knowledge, our study employed a multifaceted approach combining bioinformatics analysis of comprehensive datasets from TCGA and GEO databases with functional experiments in vitro. Our results unveiled miR-133b as a pivotal prognostic miRNA in OSCC, with overexpression significantly inhibiting the growth, migration, and invasion of OSCC cells. Through a series of molecular assays, we identified FSCN1 as a direct target of miR-133b,providing mechanistic insights into its tumor-suppressive role. Clinically, high levels of FSCN1 were associated with adverse clinicopathological features and poor survival outcomes in OSCC patients, underscoring its potential as a prognostic biomarker. Furthermore, gene set enrichment analysis revealed a link between FSCN1 overexpression and the unfolded protein response pathway, shedding light on potential therapeutic vulnerabilities in OSCC. In conclusion, our findings highlight the significance of the miR-133b/FSCN1 axis in suppressing OSCC progression, suggesting its promise as both a prognostic indicator and a target for novel therapeutic interventions. This study enhances our understanding of the complex molecular landscape of OSCC and paves the way for future clinical applications in improving patient outcomes.

Keywords: Head and Neck Squamous Cell Carcinoma; miR-133b; Transcriptome Data; Cell Invasion; Metastasis.

1. Introduction

Head and neck squamous cell carcinoma (HNSCC) ranks as the sixth most common cancer globally, affecting areas such as the mouth, throat, voice box, and salivary glands [1]. Among the various subtypes, oral squamous cell carcinoma (OSCC) is the most prevalent, making up around 30% to 50% of all HNSCC cases [2], with significantly elevated occurrence rates in South Asian and Eastern European populations [3]. Despite advancements in surgery, radiation, and chemotherapy, the 5-year survival rate for OSCC patients with advanced disease or spread to lymph nodes has seen only marginal improvement in recent decades [4, 5]. The disease's aggressive local growth and tendency to metastasize early pose significant challenges to successful treatment outcomes [6]. Given this harsh reality, there is a pressing need to pinpoint dependable prognostic markers and more effective targeted therapies. In this context, non-coding RNAs, particularly microRNAs (miRNAs), are increasingly being acknowledged for their crucial roles in cancer progression and offer promising avenues for further research and intervention. [7-9]

MicroRNAs are small, non-coding transcripts that play a crucial role in regulating gene expression in cells [10]. By binding to specific regions on target messenger RNAs, they can either promote their degradation or inhibit their translation into proteins. Depending on the cellular environment and the specific target genes, microRNAs can act as either oncogenes or tumor suppressors [11]. It is now known that more than 60% of human protein-coding genes are regulated by microRNAs, demonstrating their significant impact on maintaining cellular balance and their role in the development of diseases [12]. These regulatory networks are complex and interconnected, with individual microRNAs capable of targeting multiple genes and each gene being potentially regulated by several microRNAs [13, 14]. Abnormal expression of microRNAs has been observed in various types of cancer [15, 16], including oral squamous cell carcinoma (OSCC). These dysregulated microRNAs have been linked to the initiation, progression, drug resistance, and prognosis of OSCC, highlighting their potential as biomarkers for early detection and personalized treatment strategies [17, 18]. Furthermore, microRNAs are known to influence essential cellular functions in OSCC, such as cell proliferation, differentiation, and movement, through interactions with various signaling pathways [19]. Therefore, a thorough understanding of the expression patterns of microRNAs and their target genes in OSCC is crucial for unraveling the molecular mechanisms underlying the disease and advancing personalized therapeutic approaches [20].

Bioinformatics is a vital interdisciplinary field that combines high-throughput data to investigate gene regulation on a molecular scale, crucial for enhancing our comprehension of human diseases.In our research,we utilized public RNA-seq databases like TCGA and GEO to carry out a comprehensive bioinformatic analysis. Our goal was to identify various miRNAs that are differentially expressed (DEMs) and forecast their targets and associated biological pathways.This integrated approach is designed to furnish a solid foundation for identifying significant tumor biomarkers and potential therapeutic options with clinical relevance,thus enhancing strategies for the prevention, early detection,and treatment of oral squamous cell carcinoma (OSCC).

2. Materials and Methods

2.1. Data Acquisition and Preprocessing

Transcriptome datasets for Head and Neck Squamous Cell Carcinoma (HNSCC) were extracted from public repositories. The TCGA portal was utilized to gather miRNA and gene expression matrices from 525 tumor specimens and 44 adjacent non-malignant tissues. To validate the findings,two GEO series—GSE28100 (17 tumors,3 normals) and GSE45238 (40 tumors,40 normals)—were selected from the GEO database based on specific criteria.These criteria included the availability of both tumor and normal samples, access to raw or normalized expression data,and sufficient sample sizes for statistical analysis. All data processing was conducted in RStudio, where probe IDs were converted to gene symbols to ensure accuracy. To reduce batch effects,the ComBat algorithm from the sva package was applied. Normalization was carried out using the normalize Between Arrays function from the "limma" package. Principal Component Analysis (PCA) was then performed using the "FactoMineR" and "factoextra" packages to visualize sample clustering within the datasets.

2.2. Differentially Expressed miRNAs Screening

The analysis of differentially expressed miRNAs (DEMs) in three datasets utilized the "limma" package, setting significance thresholds at $|\log_2\text{Fold Change (FC)}| > 1$ and a P-value < 0.05. Visual representations were created through volcano plots and heatmaps using "ggplot2" and "pheatmap" packages, respectively. An overlapping analysis with a Venn diagram (Venn Diagram package) was conducted. Prognostic value was evaluated through univariate Cox proportional hazards regression to rank candidate miRNAs, leading to the creation of a forest plot for visualization. This process aimed to identify the most promising DEMs for future experimental validation. The results provide valuable insights into potential miRNA biomarkers and their associations with various diseases or conditions.

2.3. Cell Culture and Transfection

The SAS OSCC cell line was cultured in DMEM/F-12 medium with 10% fetal bovine serum and 100 U/μg/mL penicillin–streptomycin at 37°C in a 5% CO_2 incubator. Prior to treatment,cells were seeded into 6-well plates until they reached 70–80% confluence.Transfections were carried out using 50 nM of miR-133b mimic or a negative control mimic (NC) from Hippobio in conjunction with SuperKine™ Lipo3.0 reagent from Abbkine,following the manufacturer's instructions. This methodology allowed for efficient transfection of the desired substances into the cells for further experimentation.

2.4. Proliferation Assay

Cell viability was measured using the CCK-8 kit from APExBIO in the United States. Following transfection,cells were seeded into 96-well plates at a density of 1×10^4 cells per well.The CCK-8 solution was added at specified time points (0,24,48,72 hours),and after a 2-hour incubation,the absorbance was measured at 450 nm using a microplate reader.This method allowed for a reliable assessment of cell viability over time.

2.5. Wound Healing Assay

Transfected cells were collected and replated in 6-well dishes before the scratch assay.The cells were grown to 90-100% confluence and then a scratch was made using a 200-μL pipette tip. Following a PBS wash,images of five random fields per well were captured at 0 and 24 hours with a Leica DMi8 inverted microscope. The wound areas were analyzed using ImageJ software,and the closure percentage was calculated by subtracting the area at 24 hours from the initial area and dividing by the initial area,multiplied by 100%.This method allows for the assessment of cell migration and wound healing capacity.

2.6. Transwell Migration and Invasion Assays

After being transfected and left overnight without serum, the cells were prepared for migration and invasion assays.The cells were first placed in medium with 0.5% FBS before being seeded into the upper inserts of a Transwell plate.For migration, the lower chamber contained 10% FBS-supplemented medium,while for invasion,the upper membrane was pre-coated with Matrigel and dried.After 24 hours of incubation,non-migrated or invaded cells were carefully removed,and the inserts were fixed and stained.This process allowed for the observation and counting of cells in five random fields per insert.Through these meticulous steps,the researchers were able to assess the migratory and invasive capabilities of the cells following the transfection process without serum.

2.7. Target Genes Prediction

Differential gene expression was analyzed in 522 HNSCC tumors and 44 normal samples from TCGA.The study identified genes with significant changes (DEGs) using limma,with strict criteria of FDR < 0.05 and $|\log_2 FC| > 1$.Potential targets of miR-133b were predicted through databases like miRWalk and miRTarBase.The overlap between these targets and DEGs formed the candidate gene set.Survival outcomes were assessed using the OncoLnc platform by dividing patients based on gene expression levels and analyzing 5-year overall survival rates with Kaplan-Meier curves.This comprehensive approach sheds light on potential biomarkers and therapeutic targets in HNSCC.

2.8. Analysis of FSCN1 Gene Characteristics

UALCAN is an online tool that specializes in analyzing TCGA transcriptome data.For this study,the TCGA dataset was utilized to explore the relationship between the gene symbol "FSCN1" and the cancer type "HNSCC".The analysis revealed valuable insights into FSCN1 expression levels in relation to HNSCC progression.

2.9. Functional Enrichment Analysis

The study utilized GEPIA2 to identify the top 100 genes exhibiting a similar expression pattern to FSCN1.These genes were further analyzed using DAVID for Gene Ontology (GO) and Kyoto Encyclopedia of Genes and Genomes (KEGG) pathway enrichment with specific criteria. The findings were visualized using ggplot2, providing insights into the functional characteristics and biological pathways associated with these genes.

2.10.Construction of Protein–protein Interaction (PPI)Network

We used GeneMANIA (https://genemania.org) and the

STRING online database(https://string-db.org/) to construct an interactive network of *FSCN1* with other proteins.

2.11.GSEA Analysis

The TCGA-HNSC RNA-seq datasets were split into two groups based on FSCN1 expression levels to explore pathways linked to FSCN1.A ranked gene list was created using $\log_2$ fold-change values,and GSEA analysis with the Hallmark gene set collection from MSigDB was conducted using the Broad Institute's GSEA software. This approach aimed to uncover significant pathways associated with FSCN1 expression in HNSC.

2.12.Dual-Luciferase Reporter Assay

Wild-type (wt) and mutant (mut) fragments of the FSCN1 3'UTR,with the miR-133b seed-match region,were synthesized and inserted into the pmirGLO vector.This resulted in the creation of pGLO-FSCN1-3'UTR-wt and pGLO-FSCN1-3'UTR-mut constructs.SAS cells were co-transfected with these constructs along with miR-133b mimic or negative control using Hieff Trans® LipoBooster 3000.After 24 hours, luciferase activity was measured using the Dual-Glo Luciferase Assay System.The study reveals the interplay between miR-133b and FSCN1 3'UTR fragments, providing insights into potential regulatory mechanisms.This experimental approach sheds light on the molecular interactions involved in gene regulation processes.

2.13.RNA Extraction and Quantitative RT-PCR

Total RNA was extracted from SAS cells using the TRIzol reagent from Solarbio in Beijing.The cells were lysed in TRIzol,before being mixed with chloroform and centrifuged to separate the aqueous phase. The RNA was then precipitated with isopropanol,washed with ethanol,air-dried,and finally dissolved in RNase-free water.The quantity and purity of the RNA were determined using a NanoDrop spectrophotometer. Subsequently, cDNA synthesis was carried out using the HiScript IV All-in-One Ultra RT SuperMix from Vazyme in Nanjing.Real-time PCR was performed using the SupRealQ Ultra Hunter SYBR qPCR Master Mix (U+) on a suitable instrument, with U6 used as the endogenous control.The relative expression levels were calculated using the $2^{-}\Delta\Delta Ct$ method.For a more detailed understanding, refer to Table 1 for the primer sequences utilized.

Table 1. Primer sequences for RT-qPCR.

Gene	Primer Sequences (5'-3')
miR-133b-F	GCGTTTGGTCCCCTTCAAC
miR-133b-R	AGTGCAGGGTCCGAGGTATT
U6-F	CTCGCTTCGGCAGCACA
U6-R	AACGCTTCACGAATTTGCGT
FSCN1-F	GCGCCTACAACATCAAAGACTC
FSCN1-R	GAAGTCCACAGGAGTGTCGC
GAPDH-F	GACTCATGACCACAGTCCATGC
GAPDH-R	CAGGTCAGGTCCACCACTGA

2.14.Western Blotting Assay

Cells transfected with the desired genes were meticulously treated to extract the necessary proteins for further analysis.After being washed with cold PBS,the cells were lysed in RIPA buffer with a protease inhibitor cocktail, ensuring the preservation of cellular structures.Centrifugation was then used to purify the lysates and determine protein concentration through a BCA assay.Subsequently,equal amounts of protein were separated using SDS-PAGE, transferred onto PVDF membranes,and blocked with non-fat milk. The membranes were then exposed to primary antibodies, followed by HRP-conjugated secondary antibodies for detection of the target proteins.The use of ECL reagent allowed for visualization of signals,with GAPDH serving as an internal control for loading accuracy.

Table 2. Antibodies used for Western blotting.

Antibody	Dilution	Catalog	Manufacturer
FSCN1	1:5000	14384-1-AP	Proteintech
GAPDH	1:5000	60004-1lg	Proteintech
HRP-goat anti-rabbit IgG	1:5000	SA00001-2	Proteintech
HRP-goat anti-mouse IgG	1:5000	SA00001-1	Proteintech

2.15.Statistical Analysis

The experiments were conducted in a minimum of three separate biological replicates to ensure reliability.The results are displayed as mean values with standard deviations. Statistical analysis was carried out using unpaired Student's t-test for two-group comparisons and one-way ANOVA for multiple-group comparisons with GraphPad Prism 10 software.A P value less than 0.05 was regarded as statistically significant in determining the outcomes of the experiments.

3. Results

3.1. Preprocessing of Transcriptomic Data

The study assessed the impact of normalization techniques on miRNA expression using boxplots. Prior to normalization, the distribution of miRNA expression was uneven in the TCGA dataset, but post-normalization,there was improved comparability across samples.This trend was also observed in the GSE28100 and GSE45238 datasets. Following batch effect correction,PCA plots illustrated a clear separation between tumor and normal specimens in all three datasets. These findings highlight the effectiveness of normalization in enhancing the consistency of miRNA expression profiles across different datasets,ultimately aiding in the accurate classification of tumor and normal samples.

3.2. Identification of Prognostic DEMs in OSCC

Analysis of data from three different datasets, TCGA, GSE45238,and GSE28100,revealed significant changes in the expression levels of miRNAs in patients with OSCC compared to normal controls.The volcano plots depicted a total of 249 upregulated and 145 downregulated miRNAs in the TCGA dataset,36 upregulated and 49 downregulated miRNAs in the GSE45238 dataset,and 91 upregulated and 82

downregulated miRNAs in the GSE28100 dataset.Heatmaps visualized the expression patterns of the top 100 differentially expressed miRNAs from each dataset.Through Venn diagram analysis,four consistently upregulated and six consistently downregulated miRNAs were identified across all three datasets. Furthermore, Cox regression analysis identified miR-133b as the most significant miRNA associated with patient survival,with a hazard ratio of 0.62 and a 95% confidence interval of 0.44–0.86,and a p-value of 0.004.As a result,miR-133b was chosen for further investigation in the context of OSCC.

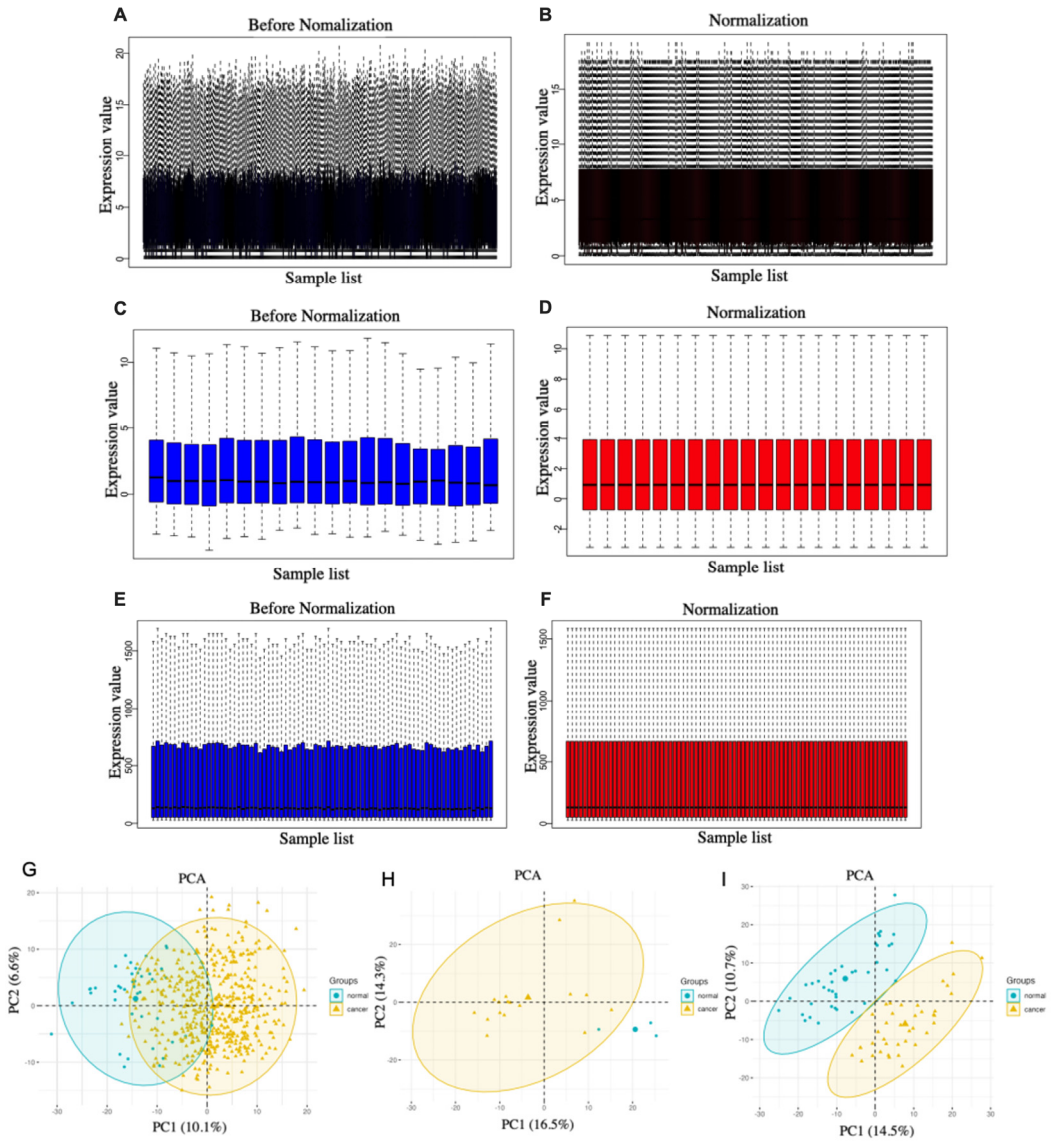

Fig 1. Preprocessing of Transcriptome Data. (A, B) Boxplots illustrating miRNA expression distributions within the TCGA dataset prior to (A) and following (B) cross-sample normalization. **(C, D)** Corresponding normalization effects visualized for the GSE28100 dataset. **(E, F)** Normalization results for the GSE45238 dataset. **(G-I)** Principal Component Analysis (PCA) scatter plots demonstrating the clear separation between tumor and adjacent normal samples across the TCGA, GSE28100, and GSE45238 cohorts after batch effect correction.

3.3. Effect of miR-133b Overexpression in OSCC Cells

Functional assays were carried out in the SAS OSCC cell line post transfection with miR-133b mimics or mimic-NC.The results indicated that the enforced expression of miR-133b significantly slowed down the growth rate of SAS cells compared to the negative control,with a substantial difference ($P < 0.0001$).Given the highly metastatic nature of OSCC,we delved further to explore the impact of miR-133b upregulation on cellular migration and invasiveness. Through wound-healing experiments,it was observed that cell lines with an overexpression of miR-133b exhibited a noticeably slower scratch closure rate in comparison to control cells. Moreover, Transwell migration assays displayed a significant reduction in the number of cells migrating through the membrane upon miR-133b overexpression. Similarly, Transwell invasion assays using Matrigel-coated inserts demonstrated a noticeable decrease in the number of invading cells in the miR-133b mimic group compared to the control group. These findings suggest that miR-133b may play a crucial role in inhibiting the proliferation, migration,and invasion of OSCC cells, opening up new possibilities for targeted therapies in the future.

3.4. Prediction and Screening of miR-133b Target Genes

Analysis of gene expression in head and neck squamous cell carcinoma (HNSCC) using data from The Cancer Genome Atlas (TCGA) revealed a total of 7616 genes that

were significantly altered,with 4551 genes being upregulated and 3065 genes downregulated.

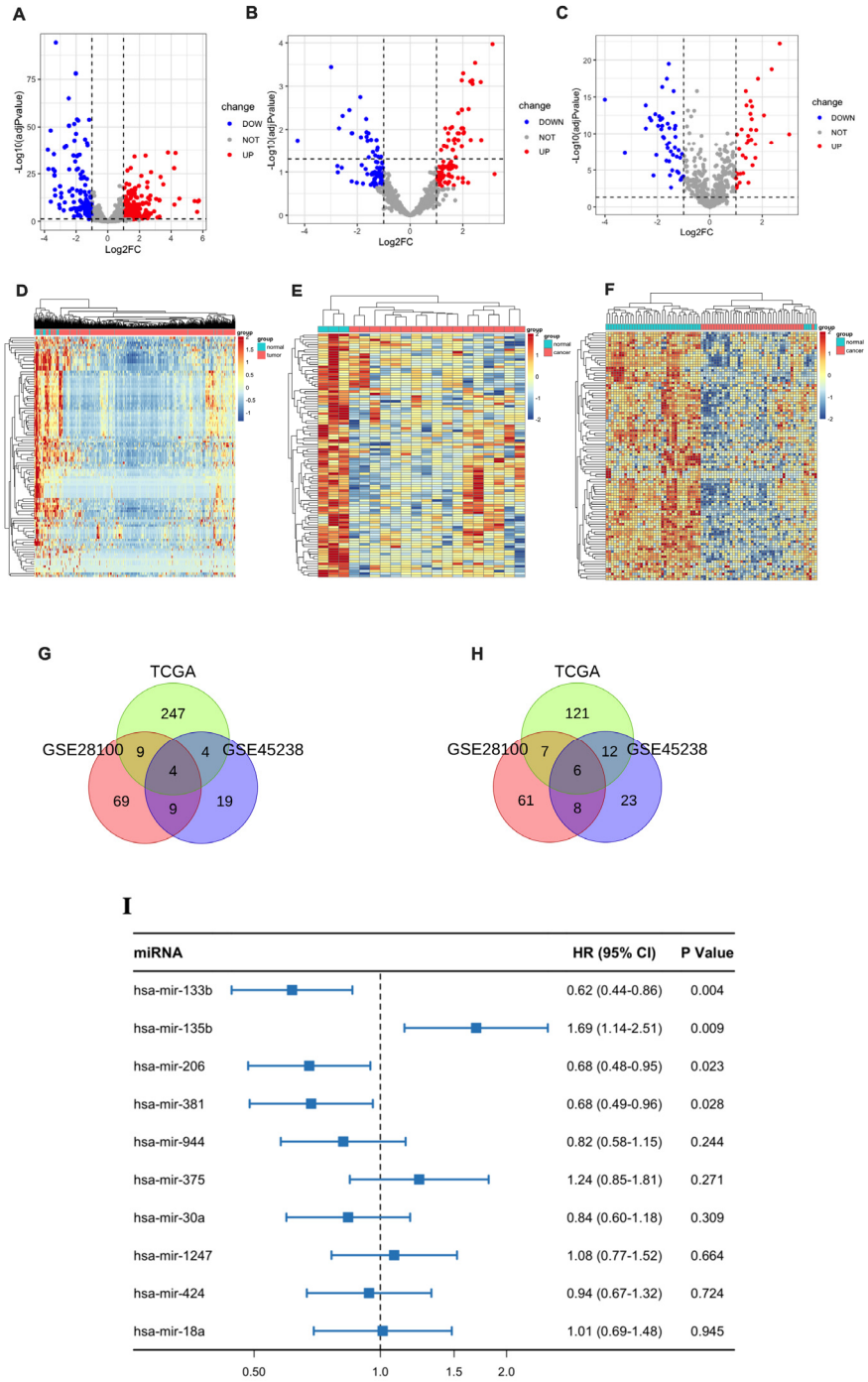

Fig 2. Screening and identification of prognostically relevant DEMs in OSCC. (A-C) Volcano plots depicting the overall landscape of differentially expressed miRNAs (DEMs) in TCGA, GSE28100, and GSE45238, respectively. Red and blue dots represent significantly upregulated and downregulated miRNAs, respectively, based on criteria of $|\log_2 FC| \geq 1$ and $P < 0.05$. **(D-F)** Hierarchical clustering heatmaps of the top 100 most significantly altered miRNAs in the three datasets. **(G, H)** Venn diagrams revealing the overlap of upregulated (G) and downregulated (H) miRNAs across the three independent datasets. **(I)** Shown as a forest plot, the univariate Cox regression findings demonstrated the association between the 10 overlapping miRNAs and patient prognosis in OSCC

By cross-referencing these genes with predicted targets of miR-133b,11 potential candidate genes were identified, including KLF15, SERPINI1, MMP9,PDE1A, FSCN1, MYPN, COL1A1,FOXL2,EGFR,TRIM71,and ZMAT4. Further analysis honed in on FOXL2 and FSCN1 as genes with a significant impact on patient outcomes,with elevated expression levels of these genes correlating with poor prognosis. Specifically,FSCN1 demonstrated a stronger association with unfavorable outcomes, indicating its potential as a prognostic marker. Given its known role in regulating actin dynamics and cancer cell mobility,FSCN1 was selected for further investigation to elucidate its mechanistic role in HNSCC progression. These findings underscore the importance of understanding the molecular mechanisms underlying HNSCC and highlight FSCN1 as a promising target for future therapeutic interventions.

3.5. Analysis of the Genetic Characteristics of FSCN1 in Tumors

Analysis conducted using the TIMER2.0 database revealed

a notable increase in the expression of FSCN1 in 11 different types of cancer when compared to normal tissues.

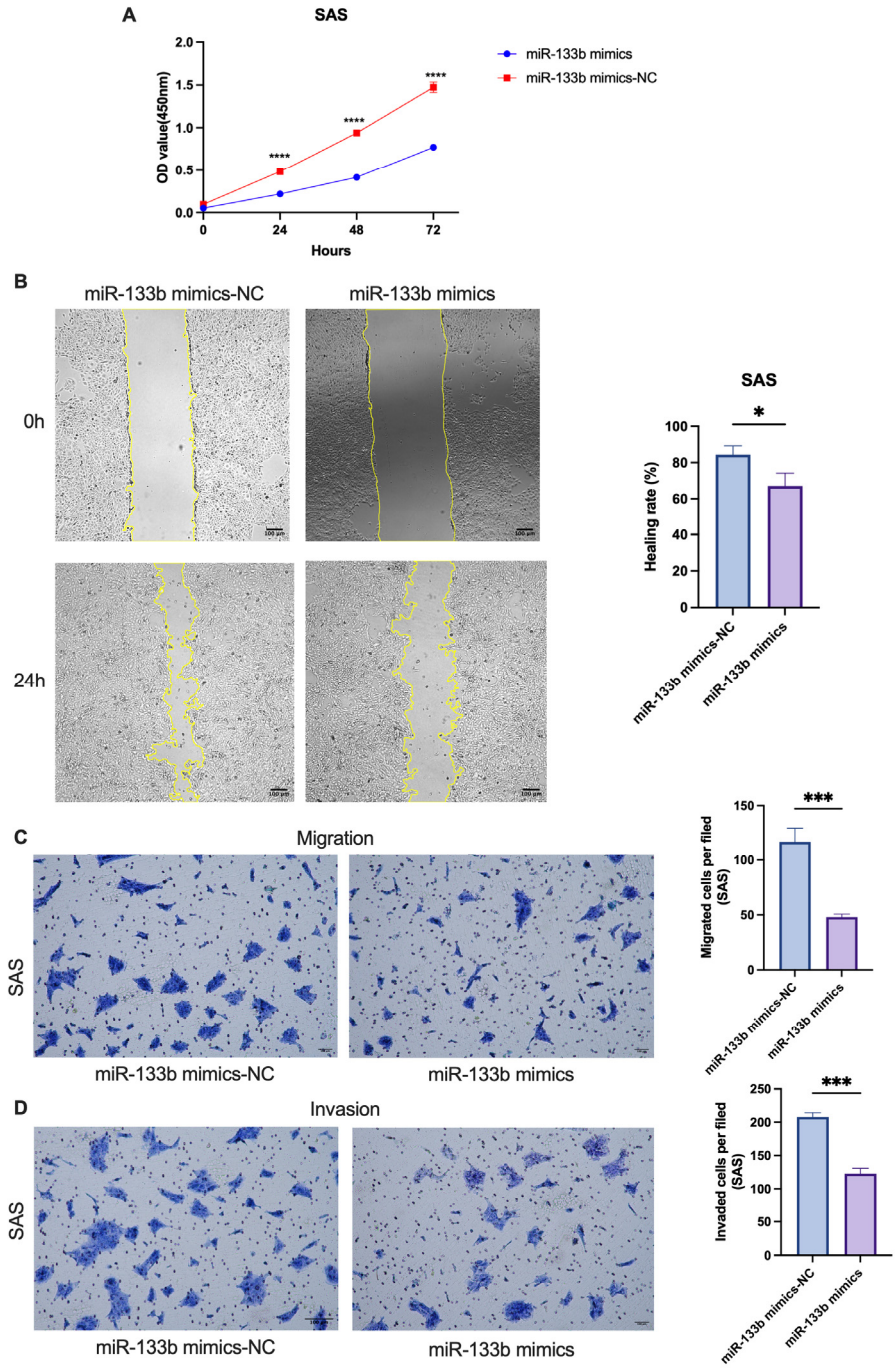

Fig 3. Impact of miR-133b overexpression on OSCC cell phenotypes. (A) CCK-8 proliferation assays showed that miR-133b mimic transfection significantly curbed the growth of SAS cells relative to the negative control. **(B)** Wound healing assays evaluating the effect of miR-133b upregulation on the migratory capacity of SAS cells, measured by scratch closure rates. **(C)** Transwell migration assays quantifying the number of cells that traversed the uncoated membrane. **(D)** Transwell invasion assays assessing the penetrative ability of SAS cells through Matrigel-coated membranes upon miR-133b overexpression. (*P < 0.05, ***P < 0.001, ****P < 0.0001)

These cancers included bladder urothelial carcinoma (BLCA), breast invasive carcinoma (BRCA), cholangiocarcinoma (CHOL), colon adenocarcinoma (COAD), esophageal carcinoma (ESCA), head and neck squamous cell carcinoma (HNSCC), kidney clear cell carcinoma (KIRC), kidney papillary cell carcinoma (KIRP), lung adenocarcinoma (LUAD), lung squamous cell carcinoma (LUSC), and stomach adenocarcinoma (STAD). This upregulation was found to be statistically significant ($P < 0.05$). Furthermore, within the TCGA dataset, FSCN1 expression was notably increased in HNSCC tumor samples in comparison to adjacent normal tissues. Subsequent analysis using the UALCAN database indicated a strong correlation between high FSCN1 expression and advanced tumor grade, higher disease stage, as well as the presence of lymph node metastasis. These findings suggest a crucial role for FSCN1 in driving the progression of HNSCC.

3.6. Functional Enrichment Analysis of FSCN1

Analyzing the functional landscape of FSCN1 involved constructing PPI and gene interaction networks. The STRING analysis revealed interacting proteins including CTNNB1,

ESPN, and ANGPTL4.

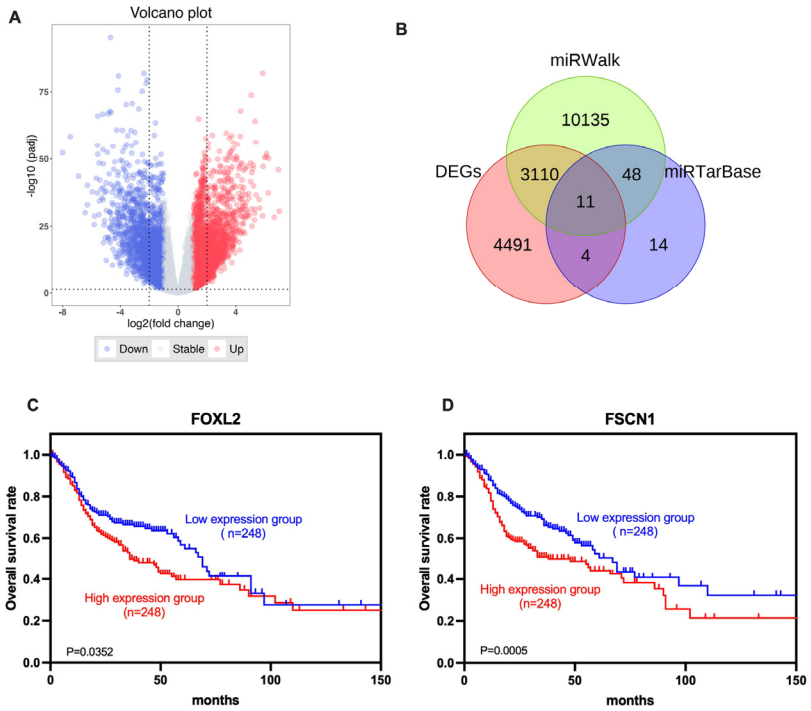

Fig 4. Prediction of miR-133b targeted regulatory genes. (A) Head and neck squamous cell carcinoma differentially related genes in TCGA. **(B)** Bioinformatics predicted that miR-133b might target different genes related to head and neck squamous cell carcinoma. **(C, D)** Kaplan-Meier curves of the 5 year overall survival frequencies according to the expression of each gene

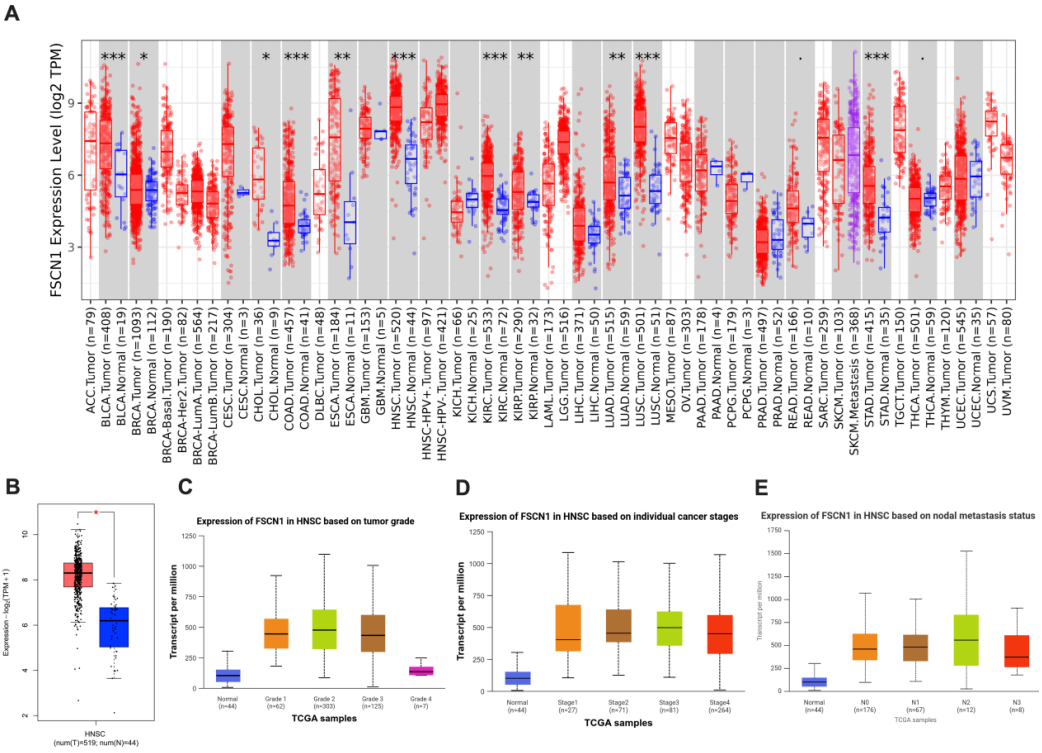

Fig 5. FSCN1 expression across pan-cancer and HNSCC cohorts. (A) TIMER2.0-derived comparison of FSCN1 mRNA levels between various cancer types and corresponding normal tissues. **(B-E)** UALCAN database analysis revealing the correlation between FSCN1 expression levels in HNSCC. (*P < 0.05, **P < 0.01, ***P < 0.001)

Further examination using GeneMANIA identified the top 20 genes closely associated with FSCN1.GO and KEGG enrichment analyses on the top 100 FSCN1-correlated genes showed significant involvement in cell adhesion, cell migration, plasma membrane, cytoplasmic components, protein binding, cadherin binding, and molecular adaptor activity. These findings suggest a crucial role of FSCN1 in various cellular processes. Additionally, KEGG pathway analysis indicated enrichment in pathways related to tumor pathogenesis, such as "Focal adhesion," "Regulation of actin cytoskeleton," and "ECM-receptor interaction." Overall, the study sheds light on the diverse functions and potential

implications of FSCN1 in cellular processes and tumor development.

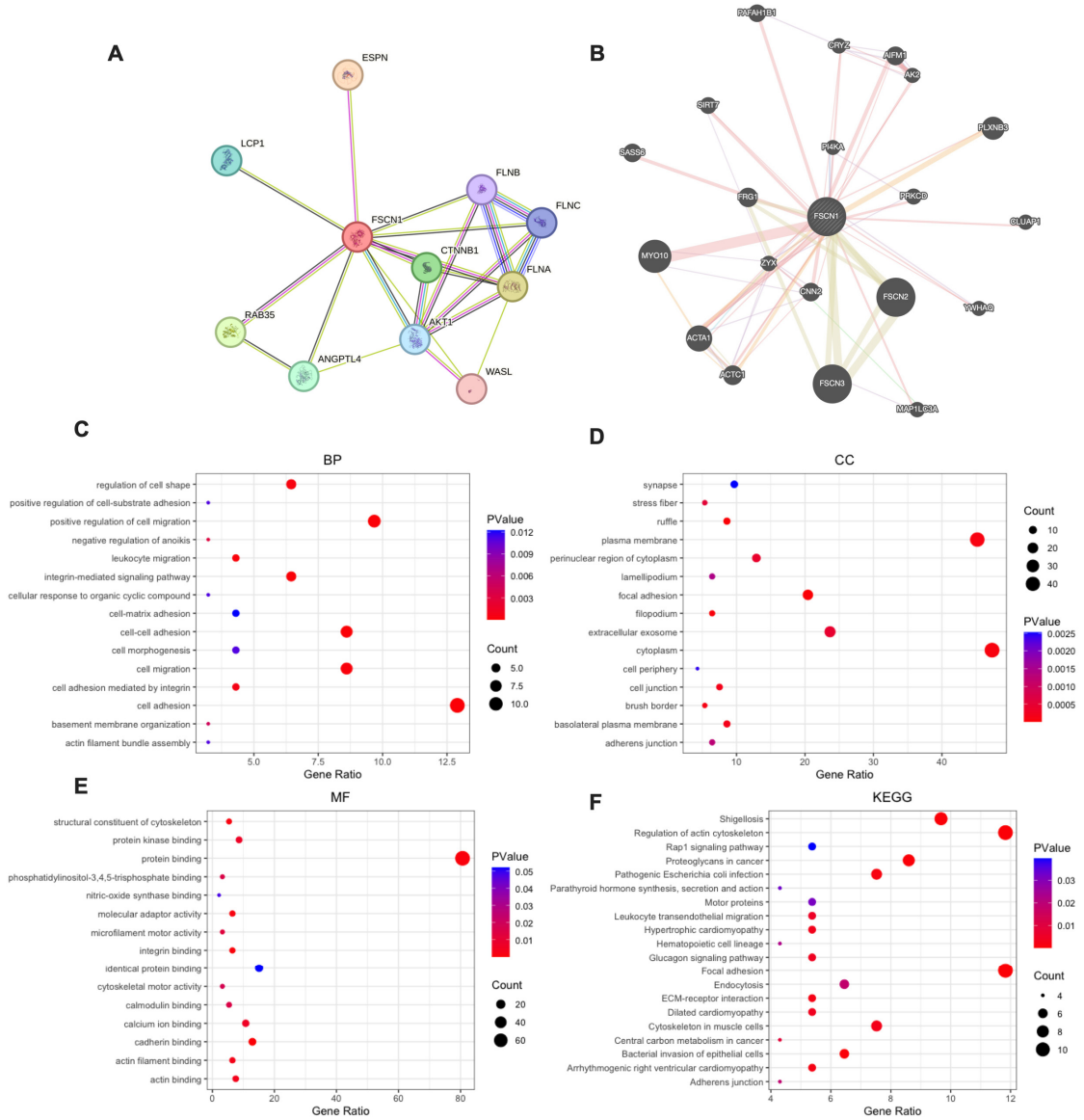

Fig 6. Enrichment of similar genes of FSCN1. (A) The PPI network shows 10 proteins interacting with FSCN1. **(B)** The gene interaction network demonstrates that the 20 most frequently changed genes are closely related to FSCN1. **(C-E)** GO analysis shows the top 15 terms significantly enriched in biological process (BP), cellular component (CC), and molecular function (MF). **(F)** KEGG analysis shows the top 20 significantly enriched signaling pathways

3.7. miR-133b Targets FSCN1 in OSCC Cell Lines

The study conducted TargetScan analysis to identify a potential binding site between miR-133b and FSCN1 mRNA's 3'UTR.To confirm this interaction,researchers generated both wild-type and mutant FSCN1 3'UTR reporter constructs.Results from dual-luciferase reporter experiments indicated that miR-133b mimic co-transfection significantly decreased luciferase activity from the FSCN1 WT 3'UTR reporter in SAS cells.Conversely,the mutant counterpart did not show a significant difference in repression. Subsequent RT-qPCR and Western blot analyses further supported these findings by showing that miR-133b overexpression led to a notable decrease in both FSCN1 mRNA and protein levels in SAS cells.These results collectively demonstrate that miR-133b directly inhibits FSCN1 expression, suggesting a potential role in suppressing OSCC tumor development and progression.

3.8. FSCN1-associated Signaling Pathways in HNSCC

GSEA analysis was conducted to investigate the impact of FSCN1 on molecular pathways in HNSCC using TCGA RNA-seq data.The results revealed that the "unfolded protein response" gene set was significantly enriched in tumors with high expression of FSCN1.This finding suggests that the unfolded protein response pathway could potentially play a key role in driving the aggressive behaviors,such as migration and invasion,that are linked to abnormal FSCN1 expression in HNSCC.

4. Conclusion

Our research utilizing a multi-omics approach and subsequent experimental validation has uncovered the regulatory significance of the miR-133b/FSCN1 axis in the development of oral squamous cell carcinoma (OSCC).

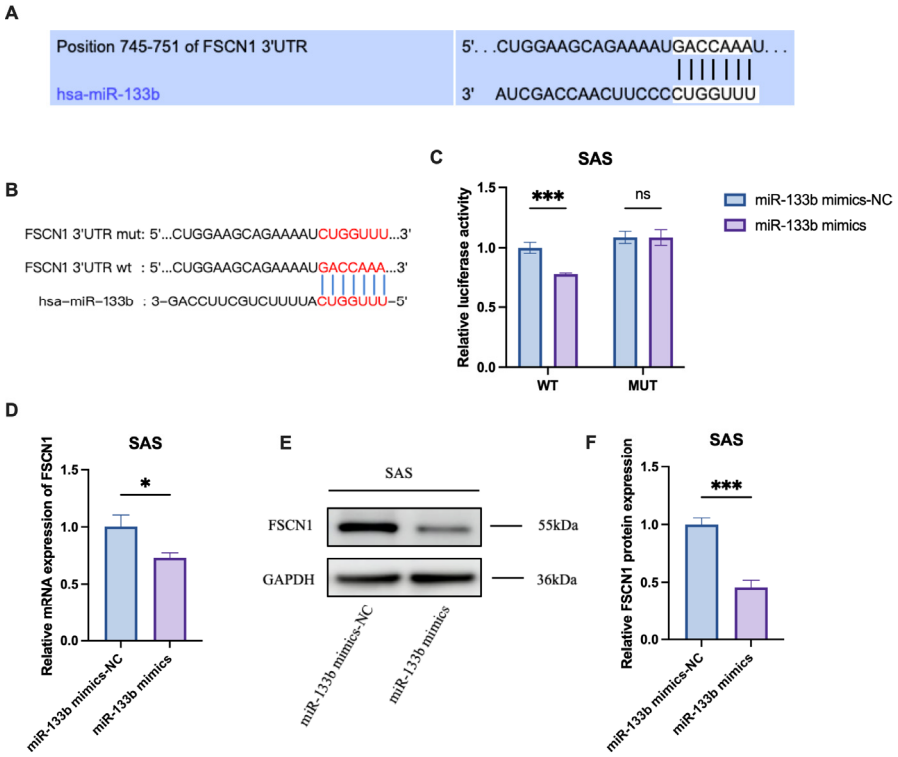

Fig 7. Validation of the direct interaction between miR-133b and FSCN1 in OSCC cells. (A) Schematic illustration of the putative complementary site between the miR-133b seed region and the FSCN1 3′-UTR. **(B)** Alignment of the wild-type (WT) and mutant (MUT) FSCN1 3′-UTR luciferase reporter constructs at the predicted interaction region. **(C)** In SAS cells, dual-luciferase reporter measurements showed that co-transfection with miR-133b mimics significantly diminished the relative luciferase activity of the WT reporter, whereas the MUT reporter remained unaffected. **(D)** RT-qPCR analysis indicated that FSCN1 mRNA levels were markedly decreased in SAS cells after transfection with miR-133b mimics compared with the negative control group. **(E, F)** Western blotting results demonstrating the downregulation of FSCN1 protein levels in response to miR-133b overexpression. (*P < 0.05, ***P < 0.001; ns, not significant)

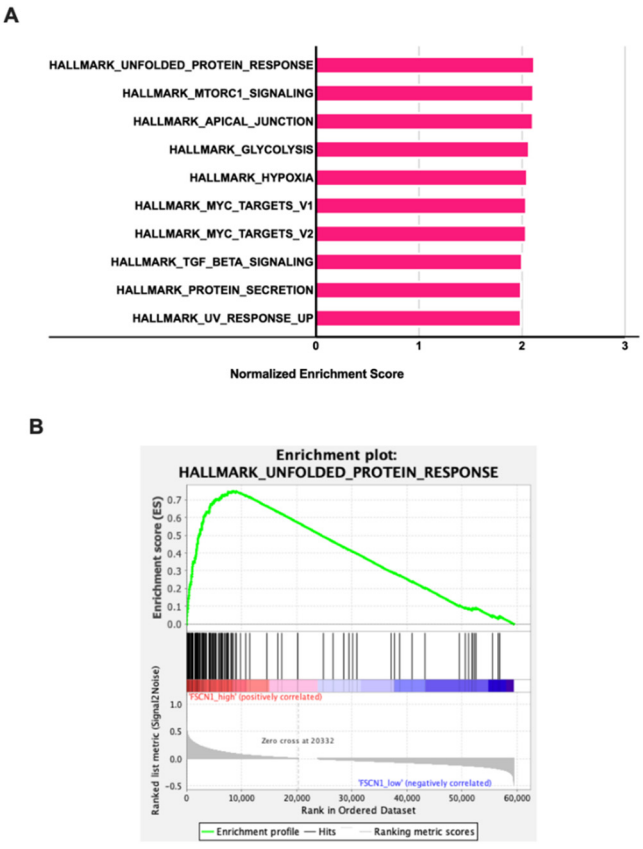

Fig 8. Identification of FSCN1-mediated signaling pathways via GSEA. (A) Bar chart displaying the top 10 Hallmark gene sets significantly enriched in the high FSCN1 expression group, ranked by Normalized Enrichment Score (NES). **(B)** Enrichment plot specifically illustrating the gene set for "Unfolded Protein Response," which exhibited the highest enrichment score

Table 3. The top 10 enriched gene sets in the high FSCN1 expression group.

Name	Normalized Enrichment Score	FDR q-Value
HALLMARK_UNFOLDED_PROTEIN_RESPONSE	2.131	0
HALLMARK_MTORC1_SIGNALING	2.121	0
HALLMARK_APICAL_JUNCTION	2.119	0
HALLMARK_GLYCOLYSIS	2.078	0.001
HALLMARK_HYPOXIA	2.062	0.001
HALLMARK_MYC_TARGETS_V1	2.052	0.001
HALLMARK_MYC_TARGETS_V2	2.050	0.001
HALLMARK_TGF_BETA_SIGNALING	2.011	0.002
HALLMARK_PROTEIN_SECRETION	2.002	0.002
HALLMARK_UV_RESPONSE_UP	2.001	0.002

Through bioinformatics analyses, we have identified miR-133b as a downregulated microRNA that holds substantial prognostic value for OSCC. By conducting luciferase reporter assays, we have confirmed that FSCN1 is a direct downstream target of miR-133b, showcasing its prominent overexpression in OSCC. Functionally, our study has demonstrated that an increase in miR-133b expression significantly hinders OSCC cell proliferation, migration, and invasion. This inhibitory effect can be attributed to the direct binding and subsequent reduction of FSCN1 at both the transcriptional and protein levels. Our findings shed light on the potential of the miR-133b/FSCN1 axis as a valuable molecular marker for subtyping and prognosis in OSCC. Furthermore, this research provides a solid experimental foundation for the development of miRNA-based targeted therapies aimed at improving clinical outcomes for patients with OSCC.

References

[1] Li, M. L., Gao, W., & Wu, Y. Y., et al. (2021). Research progress of cancer stem cell biomarkers in head and neck squamous cell carcinoma. *Journal of Clinical Otorhinolaryngology Head and Neck Surgery*, *35*(9), 854–858.

[2] Sung, H., Ferlay, J., Siegel, R. L., et al. (2024). Global Cancer Statistics 2022: GLOBOCAN Estimates of Incidence and Mortality Worldwide for 36 Cancers in 185 Countries. *CA: A Cancer Journal for Clinicians*, *74*(3), 229–263. https://doi. org/ 10. 3322/caac.21878.

[3] Sung, H., Ferlay, J., Siegel, R. L., et al. (2021). Global Cancer Statistics 2020: GLOBOCAN Estimates of Incidence and Mortality Worldwide for 36 Cancers in 185 Countries. *CA: A Cancer Journal for Clinicians*, *71*(3), 209–249. https://doi.org/ 10. 3322/caac.21660.

[4] Johnson, D. E., Burtness, B., Leemans, C. R., et al. (2020). Head and neck squamous cell carcinoma. *Nature Reviews Disease Primers*, *6*(1), 92. https://doi.org/10.1038/s41572-020-00230-2.

[5] Chi, A. C., Day, T. A., & Neville, B. W. (2015). Oral cavity and oropharyngeal squamous cell carcinoma—an update. *CA: A Cancer Journal for Clinicians*, *65*(5), 401–421. https:// doi. org/ 10.3322/caac.21280.

[6] Leemans, C. R., Braakhuis, B. J., & Brakenhoff, R. H. (2011). The molecular biology of head and neck cancer. *Nature Reviews Cancer*, *11*(1), 9–22. https://doi.org/10.1038/nrc2982.

[7] Yang, C. X., Sedhom, W., Song, J., & Lu, S. L. (2019). The Role of MicroRNAs in Recurrence and Metastasis of Head and Neck Squamous Cell Carcinoma. *Cancers*, *11*(3), 395. https:// doi. org/10.3390/cancers11030395.

[8] Dias, F., Morais, M., Teixeira, A. L., & Medeiros, R. (2018). Involving the microRNA Targetome in Esophageal-Cancer Development and Behavior. *Cancers*, *10*(12), 381. https://doi. org/ 10.3390/cancers10120381.

[9] Wang, M., Yu, F., & Li, P. (2018). Circular RNAs: Characteristics, Function and Clinical Significance in Hepatocellular Carcinoma. *Cancers*, *10*(9), 258. https://doi. org/ 10.3390/cancers10090258.

[10] Guo, M. W., Fan, Y. H., & Ren, G. D. (2025). Molecular basis of microRNA stability and degradation in plants. *Hereditas (Beijing)*, *47*(8), 944–957.

[11] Lin, S., & Gregory, R. I. (2015). MicroRNA biogenesis pathways in cancer. *Nature Reviews Cancer*, *15*(6), 321–333. https: // doi.org/10.1038/nrc3932.

[12] Chen, X., & Zhang, C. Y. (2024). Small but mighty: How ubiquitous microRNAs are reshaping life sciences. *Acta Physiologica Sinica*, *76*(5), 673–676.

[13] Ha, M., & Kim, V. N. (2014). Regulation of microRNA biogenesis. *Nature Reviews Molecular Cell Biology*, *15*(8), 509–524. https://doi.org/10.1038/nrm3838.

[14] Diener, C., Hart, M., Fecher-Trost, C., et al. (2023). Outside the limit: questioning the distance restrictions for cooperative miRNA binding sites. *Cellular & Molecular Biology Letters*, *28*(1), 8. https://doi.org/10.1186/s11658-022-00392-8.

[15] Yang, C. X., Sedhom, W., Song, J., et al. (2019). The Role of MicroRNAs in Recurrence and Metastasis of Head and Neck Squamous Cell Carcinoma. *Cancers*, *11*(3), 395. https://doi. org/ 10.3390/cancers11030395.

[16] Dias, F., Morais, M., Teixeira, A. L., & Medeiros, R. (2018). Involving the microRNA Targetome in Esophageal-Cancer Development and Behavior. *Cancers*, *10*(12), 381. https://doi. org/ 10. 3390/cancers10120381.

[17] Nair, A. S., Sujir, N., Sen, D., et al. (2026). Expression Analysis, Diagnostic and Prognostic Accuracy of microRNAs in Oral Cancer: An Overview With Meta-Analysis. *International Dental Journal*, *76*(1), 109305. https://doi.org/10. 1016/j. identj.2025.109305.

[18] Milutinovic, J., Tomic, S., Miladinovic, M., et al. (2025). Clinical Relevance of FOXP3, PD-L1, PD-1, and miR-155 Gene Expression and Genetic Variants in HPV-Negative Oral Carcinomas. *International Journal of Molecular Sciences*, *26*(15), 7218. https://doi.org/10.3390/ijms26157218.

[19] Qin, Y., Dong, X., & Li, B. (2025). Salivary miRNAs and cytokines associated with diagnosis and prognosis of oral squamous cell carcinoma. *Frontiers in Cell and Developmental Biology*, *13*, 1531016. https://doi.org/10.3389/ fcell.2025. 1531 016.

[20] Yao, M. M., Qiu, Y. L., & Liu, T. J., et al. (2025). Role of microRNA200a/141-signal transduction and transcriptional activator 4 axis in the progression of oral squamous cell carcinoma. *International Journal of Stomatology*, *52*(4), 473–483.